Egyptian Journal of Pure and Applied Science

Synthesis and characterization of poly (polyaniline/glycidyl methacrylate)/ -TiO_2 nanocomposites via gamma radiation and their uses as electroconductive material

Magda B. El-Arnaouty[1], Mona Eid[1], Mohamed Salah[1*], El-Sayed Soliman[2] and El-Sayed A. Hegazy[1]

[1]*Polymer Chemistry Department, National Center for Radiation Research and Technology, Atomic Energy Authority, Nasr City, P.O. Box 29, Cairo, Egypt,*
[2]*Chemistry Department, Factually of Science, Ain Shams University, Cairo, Egypt*

A R T I C L E I N F O

Article history:
Received 16 February 2016
Accepted 28 November 2016

Keywords:
Electroconductive material;
Polyaniline P(ANI/GMA);
TiO_2.

A B S T R A C T

polyaniline/glycidyl methacrylate-TiO_2 [P(ANI/GMA)-TiO_2] nanocomposite materials was prepared by using gamma radiation. The synthesized polymers were characterized by X-ray diffraction pattern (XRD) which proving the existence of TiO_2 nanoparticles within the composite and the peaks related to the TiO_2 nanoparticles centered at 2Θ= 25.3°, 27.5°, 37°, 38°, 41.37°, 48.1°, 54.26°, and 55.2°. The characteristic FTIR peaks of P(ANI) were found to shift to higher wave number in P(ANI/ GMA)- TiO_2nanocomposites due to interaction between TiO_2 and P(ANI/ GMA). Morphological and structural properties of these composites have also been characterized by scanning electron microscopy (SEM). The thermal stability studies using thermal gravimetric analysis (TGA) confirmed that the presence of TiO_2 leads to increase the thermal stability. The electrical conductivity measured using LCR Meter was around 10^{-3} S/cm which improves it as good electro-conductive material.

Introduction

Conductive polymers are organic polymers that conduct electricity [1]. Several applications of conducting polymers have been known like in sensors, electronic devices, batteries, and anti-corrosive additive inorganic coatings [2]. Polyaniline (PANI) is one of the most studied electrically conducting polymers due to its good processibility, environmental stability and different applications in the field of catalysis, biosensors, batteries, electronic technology and it can also be easily doped with inorganic and organic acids [3]. Polyaniline has a unique status due to the presence of reactive –NH– groups in the polymer chain flanked on either side by phenylene rings, which imparts chemical flexibility to the system and improves the possibility to a large extent [4].

Epoxy resin is one of the most important thermosetting polymers, widely used in adhesives, coatings, electronics, high performance composite materials, and aerospace industries due to its excellent mechanical and chemical properties, such as high tensile and compressive strength, good chemical resistance, and high heat distortion temperature [5].

The incorporation of inorganic fillers was achieved long ago to enhance the properties of neat epoxy nanocomposites, and they are specialty products where these inorganic fillers are dispersed in the nanoscale, and with at least one dimension of the filler phase being less than 100 nm. The incorporation of inorganic TiO_2 nanocrystals with high refractive index and wide energy gap obtaining modified polymer with new optical properties, tunable by varying the composition, size and concentration of the embedded inorganic part and better thermo- mechanical stability [6]. In order to prepare the nanoscale materials successfully, several methods have been employed. Among these methods, the γ-irradiation technique is useful and has been extensively used to generate nanoscale metals and nanocomposites at room temperature under normal pressure. Moreover, this technique is easily controlled and adaptable, and it does not contribute impurities into the matrix [7].

In this paper, P(ANI/GMA) and P(ANI/GMA)-TiO_2 nanocomposites were prepared by gamma radiation. The products were characterized by Fourier transform infrared spectroscopy, X-ray diffraction (XRD), Scan electron microscope (SEM), Thermogravimetric analysis (TGA) and electrical conductivity. The P(ANI/GMA) and P(ANI/GMA)- TiO_2 can be used as charge storage or as materials in solar cells due to their excellent photovoltaic properties.

* Corresponding author.
E-mail address: mohamed_soliman124@yahoo.com

Materials and methods

Materials

Glycidyl methacrylate (2,3 epoxy propyl methacrylate)≥ 97%(GC) and Titanium dioxide < 100nmparticle size were obtained from SIGMA-ALDRICH, Co. (USA). Aniline, Oxford laboratory, made in India. All chemicals used are of analytical reagent grade.

Experiments:

Preparation of polyaniline

20% of polyaniline was prepared by adding 20 ml of aniline to 40 ml of HCl then dissolving in 40 ml of methanol. The mixture was stirred for 2 hours at room temperature then irradiated with ^{60}Co gamma ray irradiator at irradiation dose 10 kGy.

Preparation of P(ANI/GMA)

Glycidyl methacrylate (GMA) was dissolved in methanol at a volume ratio (50:50) at room temperature as a stock solution. The prepared polyaniline was added to Glycidyl methacrylate (GMA) solution with volume ratio (80:20) then stirring for 2 hours. The mixture solution was poured into test tubes then irradiated by 10 kGy gamma rays.

Synthesis of P(ANI/GMA)- TiO_2 nanocomposites

Preparation of P(ANI/GMA) at the ratio (80:20) was carried out by adding the prepared polyanilie solution to GMA then stirring via magnetic stirrer. Through the stirring process, 0.3% nano-size titanium dioxide (TiO_2) was added to the mixture with continuous stirring for 2 hours at room temperature then the mixture was sonicated for 12 minutes. The mixtures were poured into glass dishes then irradiated by gamma rays at irradiation dose 10 kGy. The obtained polymers were dried in oven at 70°C for 24 hours.

Characterization

FTIR spectroscopy

FTIR of samples was performed according to ASTM E 1252-(02) "Standard Practice for General Techniques for Obtaining Infrared Spectra for Qualitative Analysis", using FTIR Perkin Elmer-Spectrum one in the range 400-4000 cm^{-1} which is found in Egyptian Petroleum Research Institute (EPRI).

X- ray diffraction (XRD)

XRD of samples was performed by using XRD spectrophotometer which is found in Egyptian Petroleum Research Institute (EPRI), Model (X'pert Pro), the X-ray data were recorded in the range from 4 to 80 (degree) 2θ with continuous scanning mode and scanning speed 8 (deg/min).

Thermogravimetric analysis

Thermogravimetric analysis was performed by using TGA-DSC which is found in Egyptian Petroleum Research Institute (EPRI), Model SDTQ 600 (USA), the temperature ranged from ambient temperature to 600°C at a heating rate of 10°C/min. The primary TGA thermograms were used to determine the thermal stability and rate of thermal decomposition of different nanocomposites.

Scan Electron Microscope (SEM)

JOEL JSM 5300 Scanning electron microscope-Japan, which found in Egyptian Petroleum Research Institute (EPRI) was used for investigating the morphology of different nanocomposites at high magnification and resolution by means of energetic electron beam.

Electrical conductivity measurements

Electrical conductivity measurements were performed by using LCR Meter (TEGAM), Model 3550 which is found in faculty of science, Ain Shams University.

Result and discussion

FTIR measurements

Figure 1(a) represents the FTIR spectra of P(ANI/GMA) composite, indicate the C=C stretching vibration bands which attributed to the quinonoid and benzenoid units appeared at 1602 and 1496 cm^{-1}, respectively. Stretch vibration of the N–H bond was appeared at 3353 cm^{-1} [8]. In addition, a stretching band at 1320cm^{-1} assigned to C-N was also observed [9]. The absorption band at 1719 and 1161cm^{-1} were corresponded to the ester C=O group originated from the P(GMA) and C-O stretching vibration. Three bands of C-O-C stretching, a medium intensity symmetric stretching vibration at about 1257 cm^{-1}, a medium intensity asymmetric band at 943cm^{-1}, and a strong band at 748 cm^{-1} may be attributed to the epoxide ring. There is a strong band at 692 cm^{-1} which attributed to (C-H) bending of aromatic ring [10]. The typical peaks of P(ANI/GMA) indicating the P(GMA) coating of P(ANI).

[GMA] [Pani: Polyaniline]

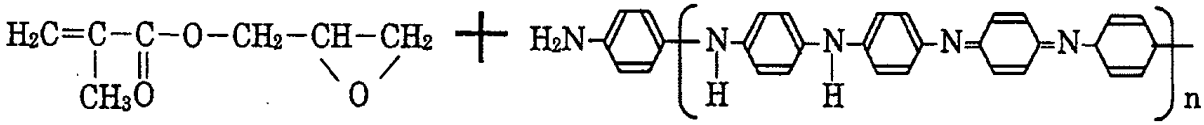

[Pani-GMA]

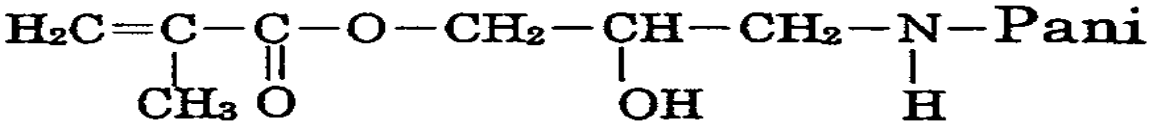

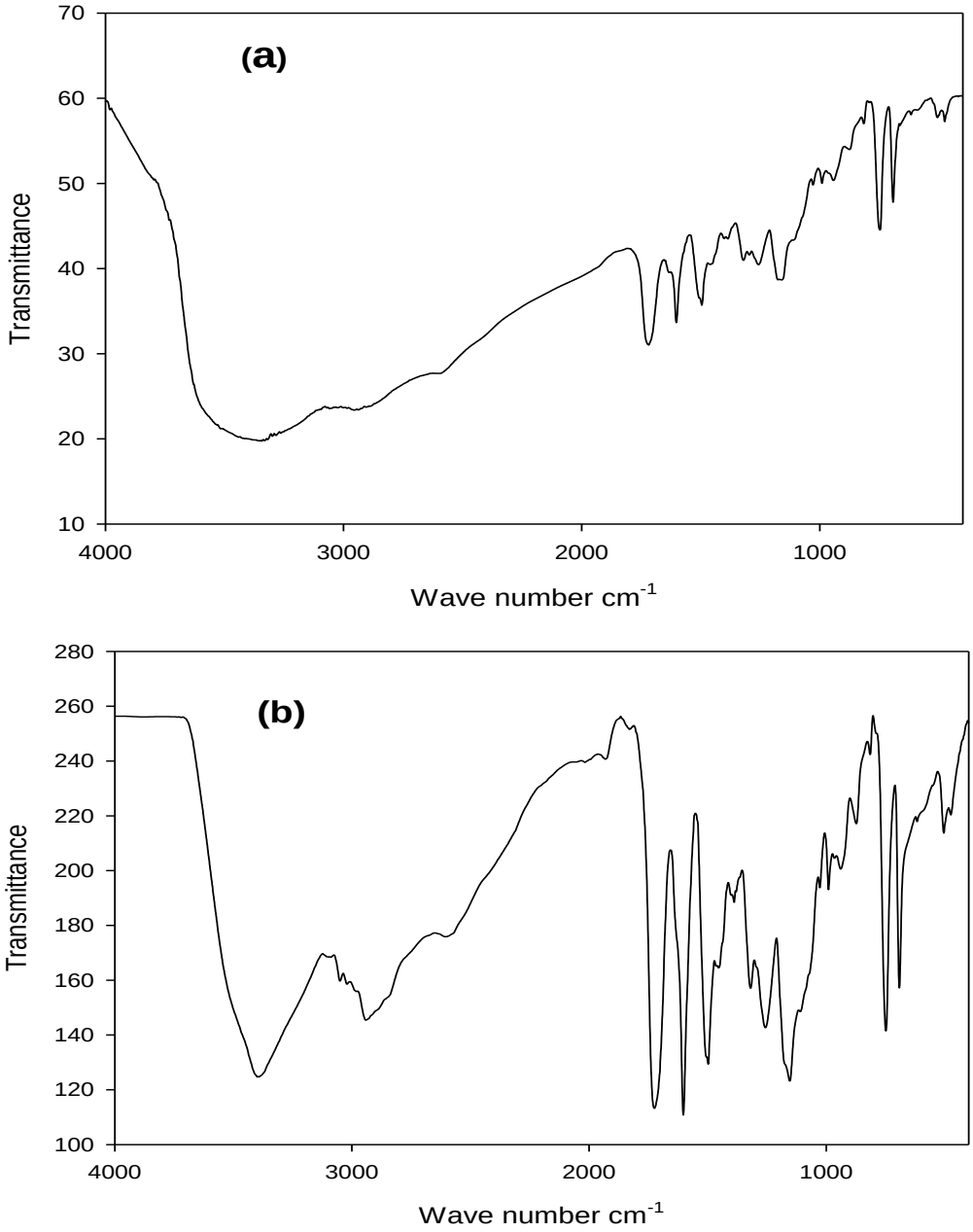

Fig (1): FTIR spectra of **(a)** P(ANI/GMA), **(b)** P(ANI/GMA)-TiO_2(0.3%).

In **Fig. 1(b)**, the P(ANI/GMA)-TiO_2 nanocomposite spectrum shows the same characteristic peaks, in addition to a peak at 670 cm^{-1} which corresponding to Ti–O stretching [11]. However, there is an evidence of peak displacement when TiO_2 nanoparticles were added to P(ANI/GMA). This displacement of 3353 cm^{-1} to 3391 cm^{-1} and 1719 cm^{-1} to 1724 cm^{-1}. It is obvious that the corresponding peaks were shifted to the higher wave number and their intensities were changed after the addition of TiO_2 nanoparticles. In addition, the methylene vibration band shifts from 2964 cm^{-1} to 2940 cm^{-1}.These significant changes suggest that an interfacial interaction exists between the P(ANI) and its inorganic counterpart of TiO_2 nanoparticles. It is known that the titanium in titania has an intense tendency to form coordination complexes with the nitrogen atoms in P(ANI) macromolecules [12].

Scan Electron Microscopy measurements (SEM)

Scanning electron microscopy is the most widely employed technique used for investigation the shape, morphology, and porosity of the polymer matrices. The SEM image of P(ANI/GMA) exhibits an amorphous surface looks like spongy shaped as shown in **Fig. 2(a)** [13]. **Figure 2(b)** shows the SEM micrograph of P(ANI/GMA)-TiO_2 nanocomposite revealed a granular structure looks like coral reefs with an interlocking arrangement. This suggests that the most of TiO_2 nanoparticles were coated with PANI [14]. The distribution and packing of TiO_2 in the P(ANI/ GMA) matrix is more uniform, and no large lumps are observed [8].

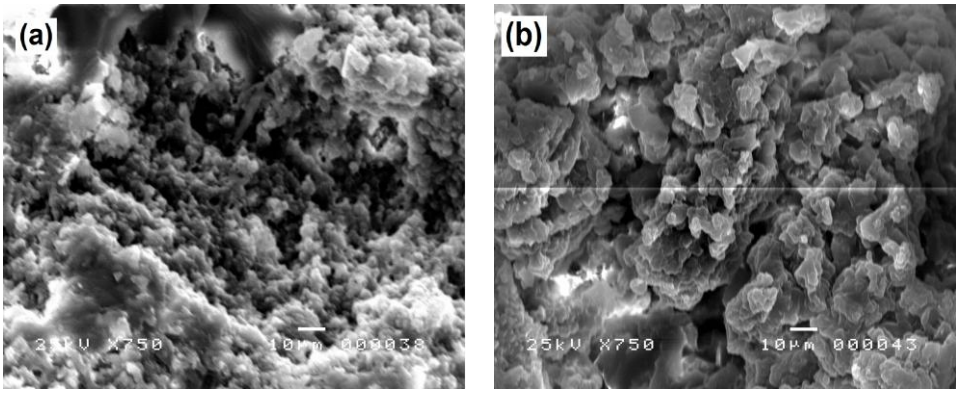

Fig (2): SEM micrographs of **(a)** P(ANI/GMA), **(b)** P(ANI/GMA)-TiO_2(0.3%)at irradiation dose 10 kGy.

X-ray diffraction measurements (XRD)

XRD was used to examine the structure of synthesized P(ANI/GMA) and P(ANI/GMA)-TiO_2nanocomposite and to investigate the effect of TiO_2 nanoparticles on the P(ANI/ GMA) structure. **Fig. 3(a and b)** shows the XRD pattern of P(ANI/GMA) and P(ANI/GMA)- TiO_2. As shown in **Fig. 3(a)**, XRD pattern of P(ANI/GMA) reveals more than one crystalline peak appeared at 2Θ = 21°, 22°, 26.7°, and 35.6° with broad amorphous peak centered at 2Θ = 16°.The peaks observed at 21°, 22°, 26.7°, and 35.6°can be ascribed to periodicity parallel and perpendicular to P(ANI) conjugation chains, respectively. The crystalline peak is indicating that HCl doped P(ANI) is not fully amorphous as well as π-π interchain stacking has improved [15-16]. According to **Fig. 3(b)**, the XRD patterns of P(ANI/ GMA)-TiO_2 nanocomposites show the characteristic peaks which improve the formation of TiO_2 nanoparticles within the composite. In case of P(ANI/ GMA)-TiO_2 nanocomposite samples of TiO_2 concentration 0.3 wt %, an amorphous peak have been appeared at 2Θ= 20°, where as the peaks related to the TiO_2 nanoparticles centered at 2Θ=25.3°, 27.5°, 37°, 38°, 41.37°, 48.1°, 54.26°, and 55.2°.

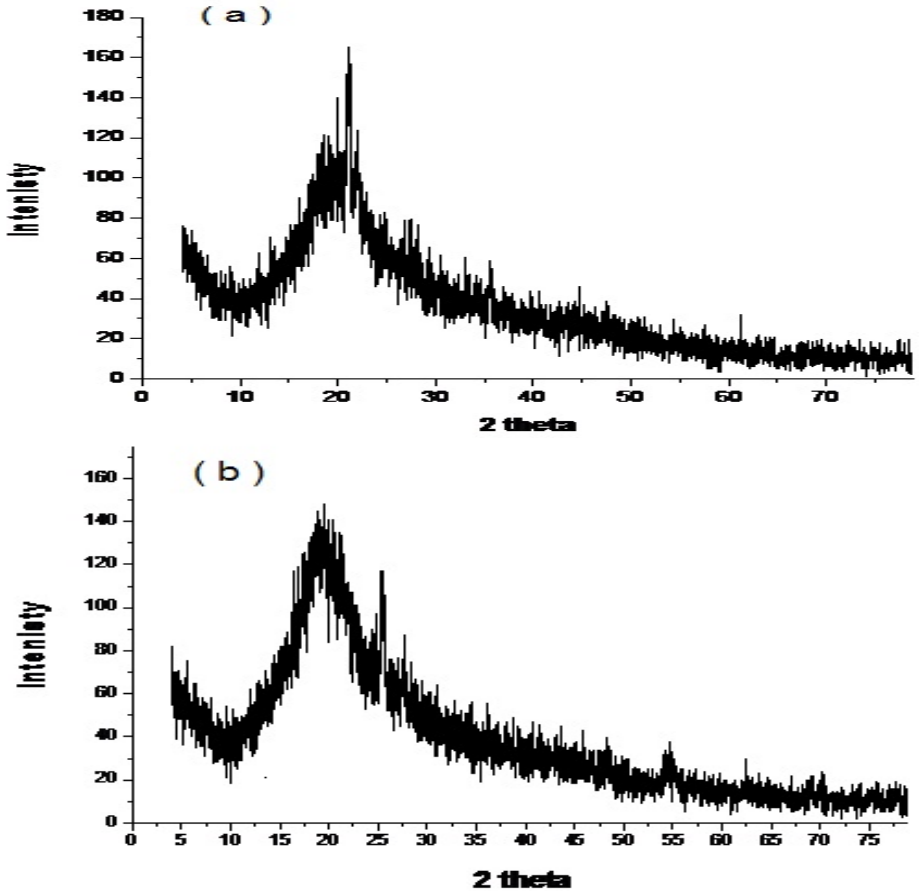

Fig (3): X-ray diffraction of **(a)** P(ANI/GMA), **(b)** P(ANI/GMA)-TiO_2(0.3%), at irradiation dose 10 kGy.

Thermogravimetric analysis (TGA)

Thermogravimetric analysis considered the most practical widely used method to illustrate the thermal stability of polymers over a wide range of temperature. **Figure 4(a)** represents the multistage thermal degradation of the P(ANI/ GMA). The first stage is up to 172°C due to the evolution of moisture with thermal decomposition percent 5.3 %. The second stage, up to 303°C, may be due to decomposition of the function groups in the side chain of the polymer with thermal decomposition percent 27.4 %. The major decomposition temperatures were within 346 and 413°C with thermal decomposition percent of 47.6 and 76.72 % respectively which may be due to the anhydride formation and basic degradation, respectively [17-18]. The final decomposition temperature at 600°C may suggest the carbonization prevails with degraded weight percent of 93.2 %.

Figure 4(b) represents the multistage thermal degradation of the P(ANI/ GMA)- TiO_2 (0.3%). The first stage up to 107°C may be due to some residual water present in the matrix with degraded weight percent of 5.3 %. The second stage and third stage, up to 201 and 302 °C respectively, which may be due to decomposition of the function groups in the side chain of the polymer with degraded weight percent 17.4% and 37.1% respectively. The major decomposition temperatures were within 347 and 394°C with degraded weight percent 61.1% and 79.4 %, respectively, which can be attributed to decomposed. The remaining weight percent at 600°C was found to be 7.2 % which may be suggested the carbonization prevails [19].

As shown in **Table 1,** it is clear that the Tmax and the Td decreased by incorporation of TiO_2 (0.3 %) into P(ANI/ GMA).From the Table, it can be also showed that the incorporation of TiO_2 decreases the maximum rate of thermal decomposition which means the increase of the thermal stability. According to the remaining weight percent in the final stage at 600°C, it can be concluded that the incorporation of TiO_2 increase the remaining weight percent for different TiO_2 contents which indicating the increase of thermal stability [13].

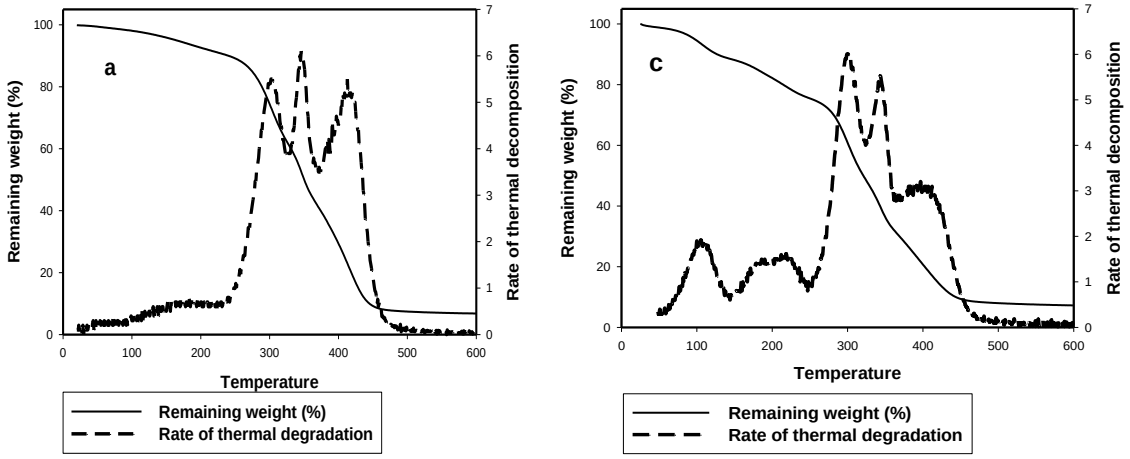

Fig (4): The TGA curve of **(a)** P(ANI/GMA), **(b)** P(ANI/GMA)-TiO_2 (0.3%) at irradiation dose 10 kGy.

Table 1: The rate of thermal decomposition (dw/dt) of P(ANI/GMA), P(ANI/GMA)-TiO_2 (0.3%) and temperatures of maximum decomposition (Tm) and start temperature of decompose (Td).

Sample description	Temperature (°C)	Rate of thermal decomposition*(dw/dt)*	T_d	T_{max}	Remaining weight (%)	Remaining weight (%) at 600°C
P(ANI/ GMA)	172	0.6	104	172	94.7	6.8
	303	5.56	243	303	72.6	
	346	6.05	326	346	52.4	
	413	5.52	375	413	23.2	
P(ANI/ GMA)-TiO_2 (0.3%)	107	1.85	60	107	94.7	7.2
	201	1.57	142	201	82.6	
	302	5.9	249	302	62.9	
	347	5.3	323	347	38.9	
	394	3.02	367	394	20.55	

Table 2: The electrical conductivity of P(ANI/GMA) and P(ANI/GMA)-TiO_2nanocomposites with different TiO_2 content 0.3% at irradiation dose 10 kGy.

Composition	Electrical conductivities (S/cm)
P(ANI/GMA)	1.343×10^{-3}
P (ANI/GMA)- TiO_2 (0.3%)	1.137×10^{-3}

Electrical conductivity measurements

Electrical conductivities of P(ANI/GMA) and P(ANI/GMA)-TiO_2 nanocomposites is described in **Table 2**. The range of electrical conductivity of P(ANI) is wide spread from10^{-10} to 10^{3} S/cm based on the acid dopant and fillers [20]. Electrical conductivity of P(ANI/GMA) and P(ANI/GMA)-TiO_2nanocomposites results show that electrical conductivity of P(ANI/GMA) decreased on adding TiO_2. This can be attributed to adsorption of –NH of P(ANI) on the surface of TiO_2 nanoparticles and bond formation in the structure. According to [13], the conductivity of the polymer depends on the nature of dopant and the inorganic materials concentration, which have an important role in conductivity of the nanocomposites [13].

Concolusion

A simple and easy route for the synthesis of P (ANI/GMA) and P(ANI/GMA)-TiO_2 nanocomposite has been demonstrated using gamma radiation. FTIR results revealed that a chemical interaction between P (ANI/GMA) and TiO_2 was established. XRD investigation indicates that, the P (ANI/GMA) has crystalline peaks beside the amorphous one. Addition of TiO_2 to P (ANI/GMA) composite show the TiO_2 related peaks. The thermal stability study of different products indicates the increase in the thermal stability by adding the TiO_2. Scan electron microscope (SEM) showed that TiO_2 nanoparticles had a significant effect on the morphology, since the TiO_2 nanoparticles are packing in the P(ANI/GMA) matrices with uniform distribution. Electrical conductivity results measured was around 10^{-3} S/cm. In conclusion, P (ANI/GMA)-TiO_2 nanocomposites could potentially use in different industrial applications including solar cells and charge storage.

References

1) **Inzelt, G. (2008).** "Chapter 1: Introduction". In Scholz, F. Conducting Polymers: A New Era in Electrochemistry. Monographs in Electrochemistry. Springer. pp. 1.
2) **Akbarinezhad, E., Ebrahimi, M. and Faridi, H. R. (2009).** Corrosion inhibition of steel in sodium chloride solution by undoped polyaniline epoxy blend coating. Prog. Org. Coat. **64**:361-364.
3) **Karim, M. R., Lee, C. J., Park, Y. -T. and Lee, M. S. (2005).** SWNTs coated by conducting polyaniline: Synthesis and modified properties. Synth. Met. **151**:131-135.
4) **Pron, A. and Rannou, P. 2002.** Processible conjugated polymers: from organic semiconductors to organic metals and superconductors. Prog. Polym. Sci., **27**:135-190.
5) **May, C. A. (1988).** Epoxy Resins Chemistry and Technology, second ed., Marcel Dekker Inc.
6) **Convertino, A., Leo, G., Tamborra, M., Sciancolepore, C., Striccoli, M., Curri, M. and Agostiano, A. (2007).** TiO_2 colloidal nanocrystals functionalization of PMMA: a tailoring of optical properties and chemical adsorption. Sens. Actuators B **126**:138-143.
7) **Karim, M. R., Yeum, J. H., Lee, M. S. and Lim, K. T. (2008).** Preparation of conducting polyaniline/TiO_2 composite submicron-rods by the γ-radiolysis oxidative polymerization method. Reactive & Functional Polymers **68**:1371–1376
8) **Strawhecker, K. E. and Manias, E. (2000).** Structure and Properties of Poly(vinyl alcohol)/Na^+ Montmorillonite Nanocomposites. Chem Mater; **12**:2943-2949.
9) **Li, X. W., Chen, W., Bian, C. Q., He, J. B., Xu, N. and Xue, G. (2003).** Surface modification of TiO_2 nanoparticles by polyaniline. Appl. Surf. Sci. **217**:16-22.
10) **Sharma, B. K., Khare, N., Dhawan, S. K. and Gupta, H. C. (2009).** Dielectric properties of nano ZnO-polyaniline composite in the microwave frequency range, Journal of Alloys and Compounds **477**:370-373.
11) **Gurunathan, K., Amalnerkar, D. P. and Trivedi, D. C. (2003).** Synthesis and characterization of conducting polymer composite (PAn/TiO2) for cathode material in rechargeable battery. Mater. Lett. **57**:1642-1648.
12) **Zhang, W. L., Piao, S. H. and Choi, H. (2013).** Facile and fast synthesis of polyaniline-coated poly(glycidyl methacrylate) core–shell microspheres and their electro-responsive characteristics. Journal of Colloid and Interface Science, **402**:100-106.
13) **Mostafaei, A. and Nasirpouri, F. (2014).** Epoxy/polyaniline–ZnO nanorods hybrid nanocomposite coatings: Synthesis, characterization and corrosion protection performance of conducting paints. Progress in Organic Coatings, **77**:146-159.
14) **Sathiyanarayanan, S., Syed Azim, S. and Venkatachari, G. (2007).** A new corrosion protection coating with polyaniline–TiO2 composite for steel. Electrochimica Acta, **52**:2068-2074.

15) **Shi, L., Wang, X., Lu, L., Yang, X. and Wu, X. (2009).** Preparation of TiO_2 / polyaniline nanocomposite from alyotropic liquid crystalline solution. Synthetic Metals, **159**:2525-2529.
16) **Long, Y., Chen, Z., Wang, N., Li, J. and Wan, M. (2004).** Electronic transport in PANI-CSA/PANI-DBSA polyblends, Physica B: Condensed Matter **344**:82-87.
17) **Li, F., Xu, X., Li, Q., Li, Y., Zhang, H., Yu, J. and Cao, A. (2006).** Thermal degradation and their kinetics of biodegradable poly(butylene succinate-co-butylene terephthate)s under nitrogen and air atmospheres, Polymer Degradation and Stability, **91**:1685-1693.
18) **Lee, K., Cho, S., Heum Park, S., Heeger, A. J., Lee, C.-W., Lee, S.-H. (2006).** Metallic transport in polyaniline. Nat. Lett., **441**:65-68.
19) **El-Arnaouty, M. B. and Eid, M. (2010).** Synthesis of Grafted Hydrogels as Mono-Divalent Cation Exchange for Drug Delivery, Polymer-Plastics. Technology and Engineering, **49**:182-190.
20) **Deng, J., He, C. L., Peng, Y., Wang, J., Long, X. and P. Li, A.S.C., Chan (2003).** Magnetic and conductive Fe_3O_4–polyaniline nanoparticles with core–shell structure. Synthetic Metals, **139**:295-301.